Green and effective synthesis of gold nanoparticles as injectable fiducial marker for real-time image gated proton therapy

Haoran Liu,[a] Naoki Miyamoto,[b,c] Mai Thanh Nguyen,[a] Hiroki Shirato,[d] and Tetsu Yonezawa[a,*]

[a]*Division of Materials Science and Engineering, Faculty of Engineering, Hokkaido University, Kita 13 Nishi 8, Kita-ku, Sapporo, Hokkaido 060-8628, Japan*

[b]*Division of Quantum Science and Engineering, Faculty of Engineering, Hokkaido University, Kita 13 Nishi 8, Kita-ku, Sapporo, Hokkaido 060-8628, Japan*

[c]*Department of Medical Physics, Hokkaido University Hospital, Kita 14 Nishi 5, Kita-ku, Sapporo, Hokkaido 060-8648, Japan*

[d]*Global Station of Quantum Medical Science and Engineering, Global Institution for Collaborative Research and Education, Hokkaido University, Kita 15 Nishi 7, Kita-ku, Sapporo, Hokkaido 060-8638, Japan*

* Corresponding author

Email address: tetsu@eng.hokudai.ac.jp (T. Yonezawa).

Catalogue

Figure S1. Synthesis route of Au NPs and alg-Au NPs. 2
Figure S2. Illustration of injectability test. 2
Figure S3. Schematic diagram of the X-ray visualization test. 3
Figure S4. TEM of Au NPs synthesized via ethanol reduction. 3
Figure S5. Viscosities of sodium alginate solutions with different concentrations. 3
Table S1. Visibility evaluation based on pattern matching scores of samples with different gold amounts under different acrylic resin thicknesses and tube currents. 4
Figure S7. TG of Au NPs-based fiducial marker and alginate hydrogel. 4
Figure S8. Size distributions of Au NPs at different time points. 5
Figure S9. UV-Vis spectra of Au NPs synthesized in alginate-only system with different sodium alginate concentrations. 5
Figure S10. TEM of sintered Au NPs processed under 600 °C. 6
Figure S11. (a) TEM and (b) size distributions of alg-Au NPs after thermal treatment. (c) Average sizes and (d) TG of alg-Au NPs before and after thermal treatment. 6
Table. S2. Visibility evaluation based on pattern matching scores of alg-Au NPs. 7
Figure S12. Relationship between pattern matching scores of alg-Au NPs and different gold amounts. 7
Figure S13. TG of alg-Au NPs-based fiducial marker and alginate hydrogel. 8
Table. S3. Size distributions of Au NPs and numbers of Au NPs collected for the calculation of size distribution. 8

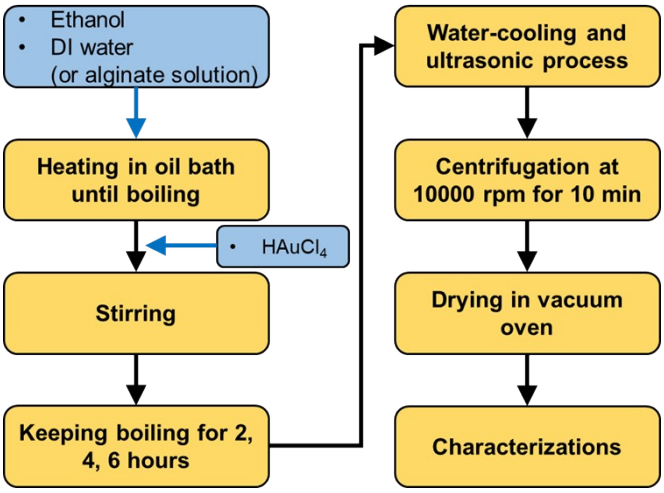

Figure S1. Synthesis route of Au NPs and alg-Au NPs.

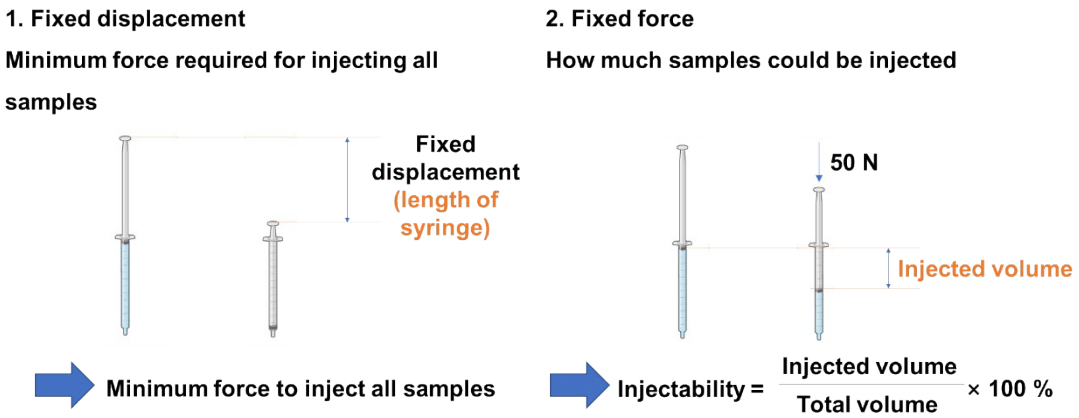

Figure S2. Illustration of injectability test.

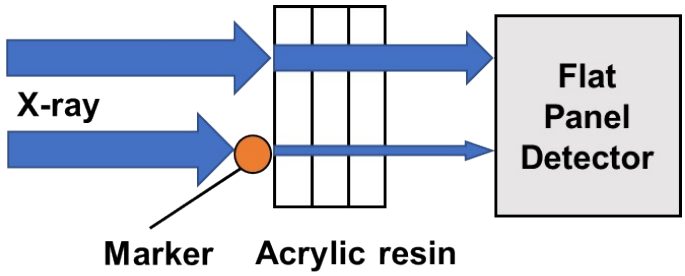

Figure S3. Schematic diagram of the X-ray visualization test.

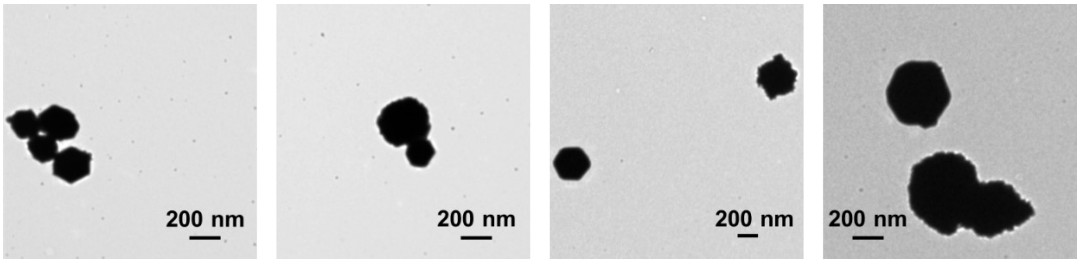

Figure S4. TEM of Au NPs synthesized via ethanol reduction.

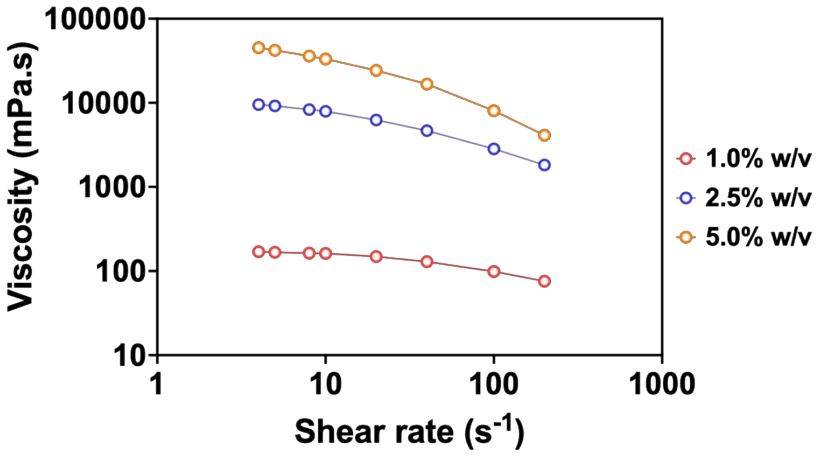

Figure S5. Viscosities of sodium alginate solutions with different concentrations.

Table S1. Visibility evaluation based on pattern matching scores of samples with different gold amounts under different acrylic resin thicknesses and tube currents.

Acrylic resin thickness (cm)	Tube current (mA)	#1	#2	#3	#4	#5	#6	#7	1.5 mm marker	2.0 mm marker
10	50	80.97	82.04	89.17	78.93	92.47	87.84	97.65	90.54	94.62
10	80	88.76	89.75	93.31	88.46	96.33	93.20	100	95.25	97.27
15	50	42.89	49.17	61.63	43.76	75.74	60.28	83.34	66.66	81.32
15	80	61.70	66.79	74.31	63.44	84.75	72.75	92.49	80.27	89.27
20	50	2.40	1.41	1.73	1.00	32.79	2.08	39.23	25.20	41.62
20	80	16.75	24.95	31.49	4.47	50.76	31.22	58.79	43.21	57.01
20	160	37.60	39.80	51.84	29.25	70.45	46.57	79.57	63.51	72.60

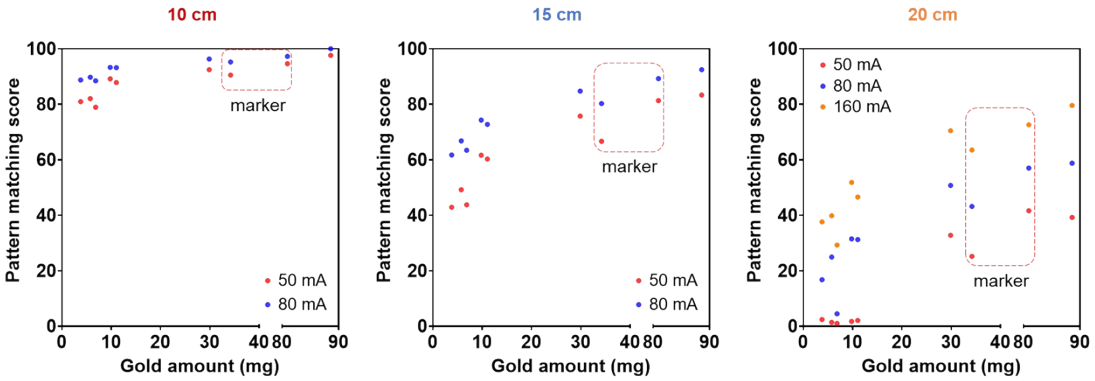

Figure S6. Relationship between pattern matching scores of Au NPs and different gold amounts.

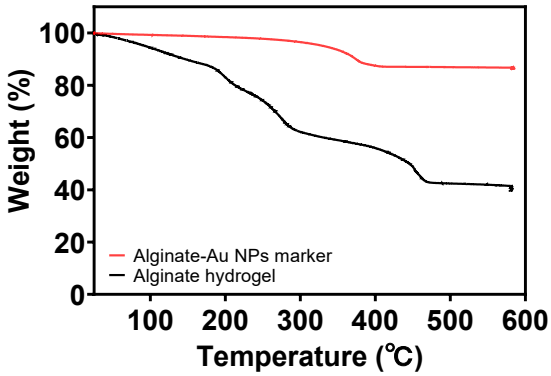

Figure S7. TG of Au NPs-based fiducial marker and alginate hydrogel.

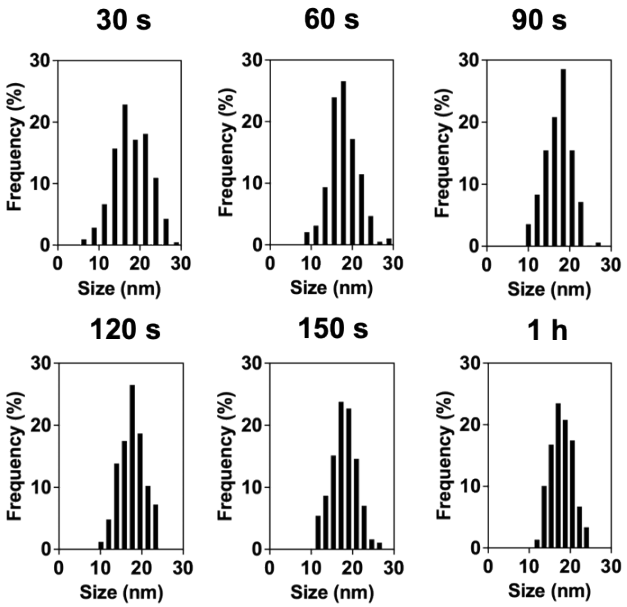

Figure S8. Size distributions of Au NPs at different time points.

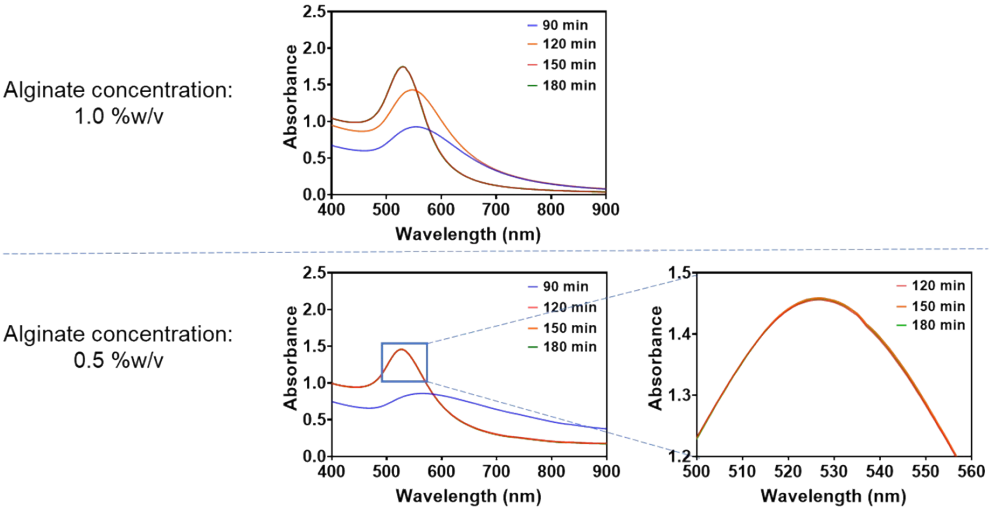

Figure S9. UV-Vis spectra of Au NPs synthesized in alginate-only system with different sodium alginate concentrations.

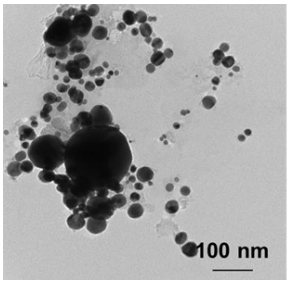

Figure S10. TEM of sintered Au NPs processed under 600 °C.

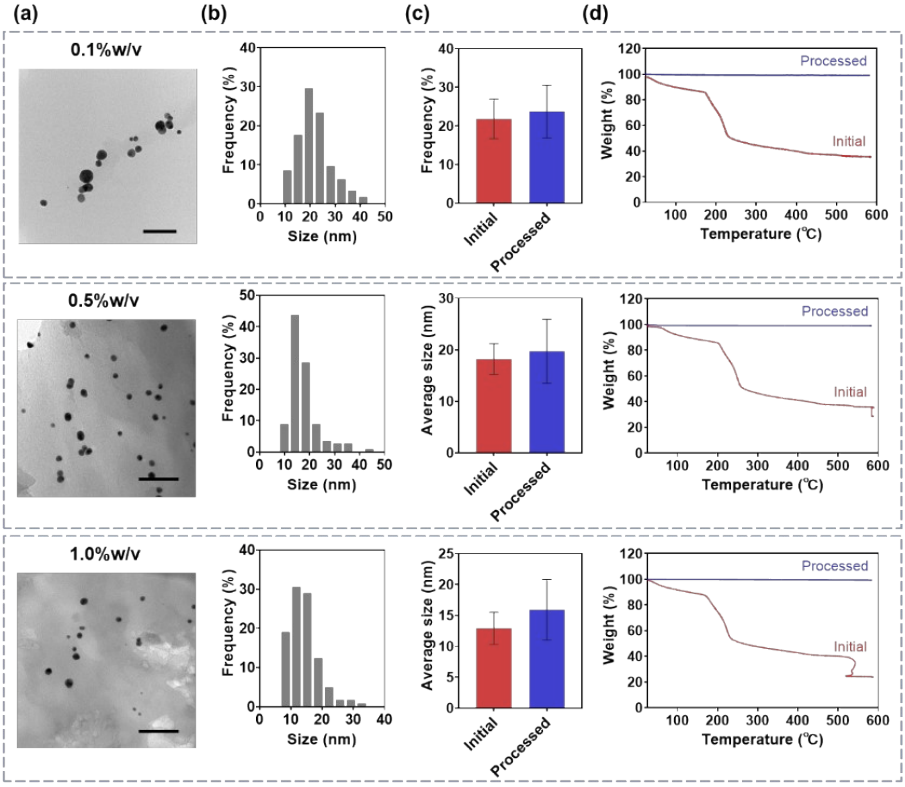

Figure S11. (a) TEM and (b) size distributions of alg-Au NPs after thermal treatment. (c) Average sizes and (d) TG of alg-Au NPs before and after thermal treatment.

Experimental steps for TGA:

- Temperature: 25-600 °C
- Temperature rate: 1 °C/min
- Hold time (600 °C): 2 h
- Atmosphere: air

Table. S2. Visibility evaluation based on pattern matching scores of alg-Au NPs.

Thickness (cm)	Current (mA)	Alg-Au NPs synthesized in different concentrations of alginate aqueous solutions									Gold ball markers	
		0.1% w/v			0.5% w/v			1.0% w/v				
		#1	#2	#3	#4	#5	#6	#7	#8	#9	1.5 mmφ	2.0 mmφ
10	50	76.11	72.72	75.84	75.84	73.34	76.98	74.15	76.67	77.17	71.65	76.07
10	80	78.47	76.48	78.08	78.08	75.93	78.08	76.83	78.41	78.78	75.63	78.02
15	50	64.4	54.57	67.17	67.17	53.3	66.54	55.17	67.47	65.96	51.95	61.03
15	80	72.04	67.02	72.6	72.6	64.45	71.21	67.06	71.92	73.97	60.6	68.88
20	50	35.85	24.1	30.59	30.59	28.01	31.66	19.17	40.15	34.43	23.11	27.48
20	80	50.72	36.76	47.78	47.78	32.03	49.77	37.26	55.76	49.19	31.63	48.49
20	160	60.63	56.87	58.03	58.03	53.97	60.64	50.89	62.63	63.86	47.02	53.20

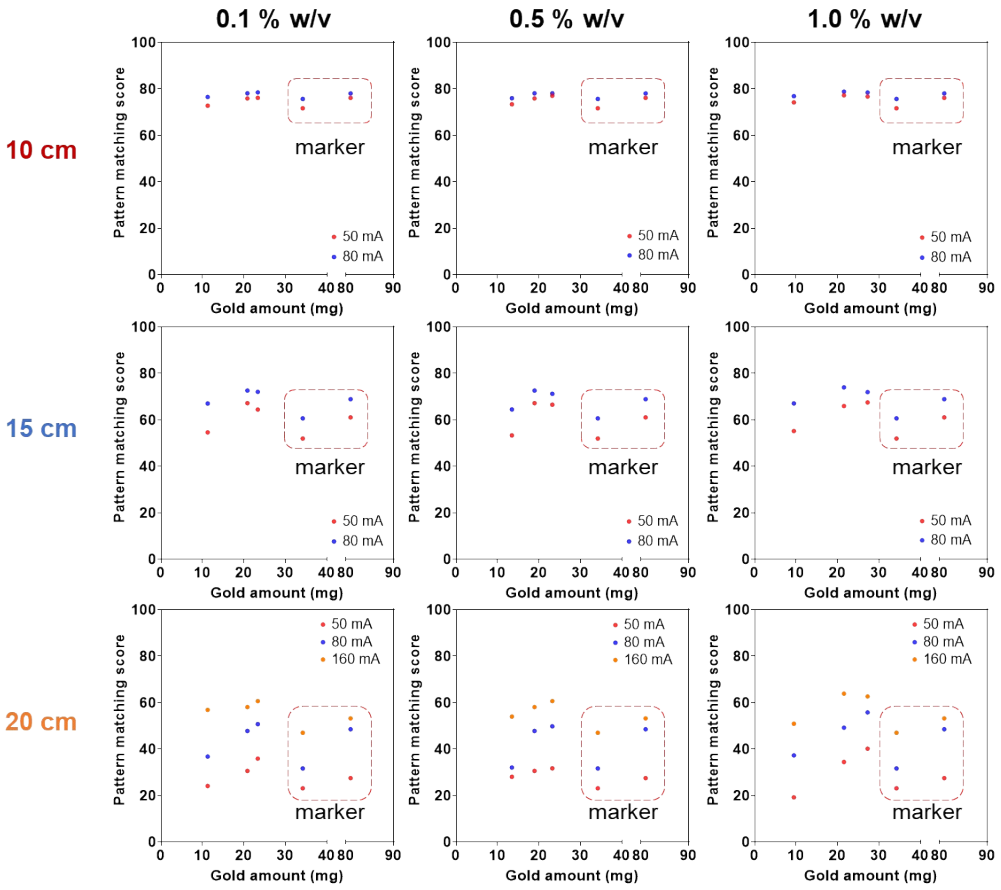

Figure S12. Relationship between pattern matching scores of alg-Au NPs and different gold amounts.

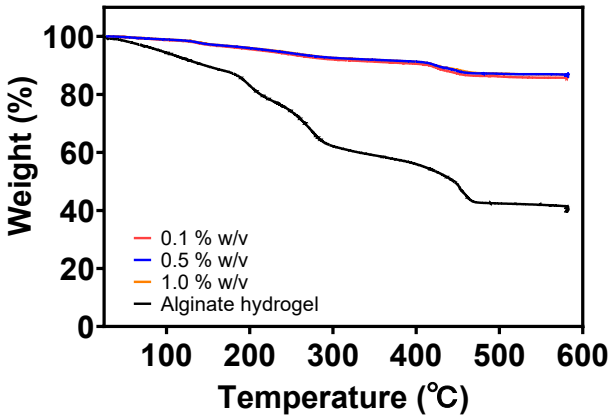

Figure S13. TG of alg-Au NPs-based fiducial marker and alginate hydrogel.

Table. S3. Size distributions of Au NPs and numbers of Au NPs collected for the calculation of size distribution.

Figure	Number of Au NPs for size distribution calculation	Average size (nm)	Standard deviation (nm)
Figure 2(c)	109	242.5	55.4
Figure 7(c)-0.1%	135	21.8	5.1
Figure 7(c)-0.5%	106	18.2	3.0
Figure 7(c)-1.0%	113	14.1	3.5
Figure 9(b)-30 s	179	19.2	4.3
Figure 9(b)-60 s	183	18.9	3.6
Figure 9(b)-90 s	168	18.3	3.2
Figure 9(b)-120 s	166	18.6	3.1
Figure 9(b)-150 s	185	18.8	3.2
Figure 9(b)-1 h	149	18.8	2.7
Figure S11(b)-0.1%	176	23.7	6.8
Figure S11(b)-0.5%	132	19.7	6.2
Figure S11(b)-1.0%	121	15.9	4.9